Civil Engineering Beyond Limits 1 (2027) 11168

Civil Engineering Beyond Limits

journal home: www.acapublishing.com/journals/1/cebel

Research Article

Structural Response and Local Alternate Load Path Assessment of an Aging Steel Truss Railway Bridge: A Computational Study of Hardinge Bridge, Bangladesh

Md. Shahriar Reza[1], Md. Mahabub Rahman[*,2], Nirmal Chandra Roy[2], Anik Kumar Debnath[3]

[1]Lecturer, Department of Civil Engineering, Hajee Mohammad Danesh Science and Technology University, Dinajpur, 5200, Bangladesh
[2]Assistant Professor, Department of Civil Engineering, Hajee Mohammad Danesh Science and Technology University, Dinajpur, 5200, Bangladesh
[3]Graduate Student, Department of Civil Engineering, Hajee Mohammad Danesh Science and Technology University, Dinajpur, 5200, Bangladesh

Keywords

FEM,
OpenSeesPy,
Hardinge bridge,
Structural response,
Demand/capacity ratio.

Abstract

The structural response and load transfer behavior of steel railway bridges under representative railway loading are systemically evaluated for aging steel railway bridges. This study is a three-dimensional finite element analysis of a representative 345ft span of the old Hardinge Bridge, Bangladesh, using OpenSeesPy. The geometry and structural configuration of the bridge were based on the available historical bridge records and published information, and representative properties of the structural-steel were assumed where direct material-test data were not available. The numerical model takes into account the dead load and an idealized railway loading configuration. The structural response was assessed by calculating vertical displacement and maximum axial stresses, and deterministic local alternate-load-path simulations were conducted by removing three members and observing the redistribution of stresses. The maximum mid-span displacement calculated for the selected baseline model was about 4.02 inch. The largest peak axial stress magnitudes were found in the lower-chord and some diagonal members. Member removal caused significant redistribution of axial demand in neighboring members, such as a tension to compression stress reversal in one member studied. The demand to capacity ratios were then calculated based on the adopted tensile yield criterion and theoretical buckling resistance of compression members. The results show that the investigated members were not exceeded in the idealized model in terms of elastic/yield or buckling resistance. The results should be viewed as a preliminary numerical evaluation of the current structural condition of the Hardinge Bridge, as the model has not been validated with field measurements.

1. Introduction

Railway bridges are crucial parts of transport infrastructure, designed to facilitate smooth transport of passengers or cargo across various natural or man-made obstacles. Amongst the different types of bridges, steel truss bridges have been widely used for railway systems because of their structural efficiency, high strength to weight ratio, and low amount of material necessary to span large distances [1-2]. Many of these rail bridges were constructed in the late 1800s and early 20th century and are still in use. Many of these structures were constructed several decades ago, have exceeded their original design lives, and are now exposed to increasing traffic demands and environmental deterioration that can present significant issues in terms of monitoring / maintenance and eventual failure.

Fatigue damage may occur in steel bridges in service because of the repeated loading from trains, and is more likely as the bridge ages. Fatigue cracks typically start in connections, at riveted joints or at other stress concentration locations and grow slowly under cycling loading conditions [3-4]. It is recognized that fatigue is one of the key mechanisms of deterioration in historic steel railway bridges and several studies have been undertaken to substantiate this. For example, Zhao et al. (2021) [5] explained that parameters such as the number of train loads are very important for stress ranges in truss members that can be used to initiate and propagate cracks for detail sensitive to fatigue. Likewise, Deng et al. (2022) [6] pointed out that the damage of fatigue accumulation in bridge connections can cause a decrease in the structural reliability of the bridges and also result in a shorter residual service life of aging railway bridges. The presence of redundancy is another critical property for structural safety in steel railway truss bridges. This is known as "structural redundancy," and implies that if the structure fails, it can still carry loads by another load path. The majority of historic truss bridges were built as statically determinate bridges without excessive redundancy, and so the loss of a single critical member can lead to a partial or even total collapse of the structure [7-8]. Some recent works have looked into the issue of redundancy and robustness in steel truss bridges as a result of this situation. Li et al. (2019) [9] have conducted a study on alternate load-path in a structural steel truss bridge and demonstrated that the extreme stresses of adjacent structural elements can occur when certain members are lost. In another study, Fu and You (2019) [10] studied the failure propagation mechanisms of truss bridges and found that local failure could result in the progressive collapse if there was not enough load redistributing capacity. Engineers have determined the structural response of bridge systems under realistic loading scenarios in a series of progressively more complex and accurate computational models. Numerical simulation methods and finite element modeling are employed to evaluate the deflection behavior and stress distribution,

*Corresponding Author: mmr.civil@hstu.ac.bd
Received 25 Jul 2026; Revised 11 Sep 2026; Accepted 15 Sep 2026
https://doi.org/10.36937/cebel.2027.11168

as well as the structural performance under moving train loads [11-12]. These methods are particularly effective for heritage bridges, where experimental tests or full-scale loading tests are not feasible, and they can be used to assess the structural integrity and safety of these historic structures in a cost effective and non-invasive manner. In addition, it is straightforward to evaluate the redundancy behavior in member-failure scenarios in the simulation with the numerical approaches.

As a result, structural health monitoring (SHM) systems have been increasingly used for the monitoring of aging bridges. These sensors can be installed on a bridge to measure the strain, displacement and vibration responses of the bridges as trains pass over them, thereby providing information on structural performance and potential damage [13-14]. Recent studies have also looked into using machine learning to find damage to bridges and assess their condition. In these studies, it is demonstrated that machine learning can detect structural issues and foresee when maintenance is required [15-16]. However, detailed computational assessments integrating structural response and local alternate-load-path behavior remain limited for historic railway steel bridges in developing regions. As with many of these bridges, they continue to serve the public despite its growing use, with no detailed structural assessment or advanced monitoring systems. One of them is Hardinge Bridge, a steel truss railway bridge over Padma River, Bangladesh, which is over 100 years old and of importance. So far, systematic numerical studies with regard to the structural behavior, the redundancy features of the bridge and the response to train loading have been relatively scarce, although bridges play a crucial role in the national railway systems.

The prior studies of steel truss railway bridges are focused on fatigue evaluation, structural health monitoring, or simulation of individual bridge components. However, very few studies have been performed that have been integrated with structural analysis to redundancy and failure propagation assessment for historic railway bridges in maintaining areas of the world. Specifically, the structural response and load-redistribution mechanism of century old railway truss bridges loaded with modern trains remains to be investigated. To bridge this gap, here we develop a computational framework to enable the evaluation of the structural response of the Hardinge Bridge under realistic railway loading situations. Research involves an examination of performance under loads, member failure, and redundancy of the bridge. The outcomes will contribute to shedding light on the structural behavior of aging steel rail bridges and provide a preliminary computational framework for identifying members associated with substantial load redistribution and for supporting subsequent detailed inspection and assessment.

2. Materials and methods

2.1. Research framework and structure of the study

Through a computational modeling framework, this study evaluates the structural performance, and redundancy behavior of the historic steel railway bridge Hardinge Bridge. The method combines geometric modeling, finite element structural simulation, and redundancy analysis under simulated railway loading conditions. This is a common multistage approach employed by many in the structural evaluation of aging steel bridges [17-19].

2.2. Description of the bridge and structural data

The study considers the Hardinge Bridge, a riveted steel truss railway bridge constructed in 1915 over the Padma River in western Bangladesh. The main structural features of this bridge are as follows:

- ✓ Total length of the bridge: ≈5940 ft (≅1810 m)
- ✓ Number of spans: 15
- ✓ Span length: 345 ft (≈105 m) per span
- ✓ Deck width: 32 ft
- ✓ Elevation: Approx. 49 ft above sea level
- ✓ Structural system: steel through truss
- ✓ Railway configuration: double broad-gauge tracks
- ✓ Structural components: top chords, bottom chords, diagonals, verticals, crossbeams, and longitudinal stringers

These structural characteristics were used as the principal inputs for geometric modeling and structural analysis. Structural dimensions and material properties were derived from historical drawings, bridge inspection reports, and literature pertaining to similar steel truss bridges. The general at site view and the shape dimensions of Hardinge Bridge are shown in Figs. 1a-d.

The historical records of this study were used mostly for defining the bridge geometry, member arrangement, span configuration and structural system. Original mill certificates, material-grade specifications and mechanical test results performed in situ for the steel were not available; material parameters used in the numerical model are explicitly different from historically documented bridge information.

(b)

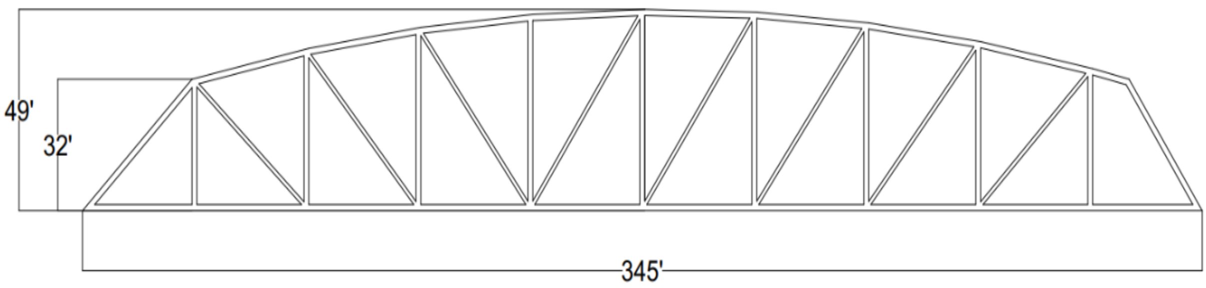

(c)

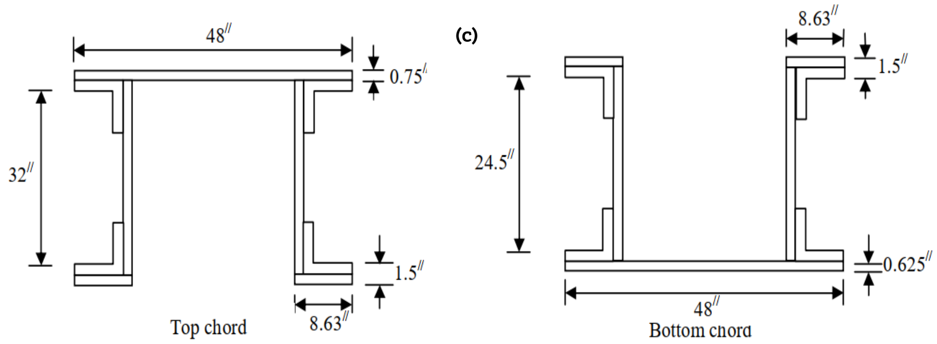

(d)

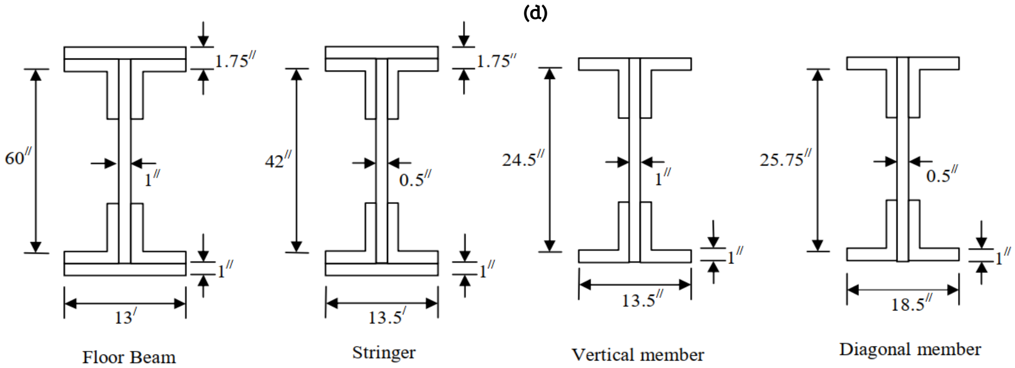

Figure 1. (a) Original site view, (b) Single span side view, (c) Cross sectional details of top chord and bottom chord and (d) Cross section details of different types of members in Hardinge Bridge

2.3. Modeling of geometric elements

A three-dimensional finite element model of the bridge was created in OpenSeesPy using three-dimensional trusses. The geometry of the bridge was modeled by specifying the coordinates of the nodes, the connections between the members, and the geometry of the cross sections of the main structural elements such as chord members, diagonal members, vertical members and floor beams. The bridge was idealized as a truss, where structural members act as truss elements and topology is defined by their nodal interactions. The three dimensional modeling however, has the benefit of guaranteeing the accuracy of the bridge behavior that can be replicated to the transmission of load to the truss members to ensure structural integrity and the performance of the bridge under load conditions is accurately assessed.

2.4. Finite element structural analysis

2.4.1. Numerical modeling

The structural response of the bridge was quantified using Finite Element Analysis in python through OpenSeesPy framework. OpenSeesPy is the Python interface to the OpenSees finite-element framework and enables scripted structural modeling and analysis. [20]. In finite element model:

- ❖ Nodes are truss joints.
- ❖ Elements – Steel members.
- ❖ This specifies the material behavior with linear elastic properties of steel.
- ❖ Boundary conditions simulate the support conditions on the bridge.

The idealization of the main truss members as axial truss members is appropriate for the primary chord, diagonal and vertical members since the force of the primary chord, diagonal and vertical members is their dominant response under the idealization adopted. The floor beams and the longitudinal stringers were modelled as beam-column elements that were able to reproduce flexural and shear deformation and to offer a physically plausible load transfer path from the railway loading system to the main trusses.

2.4.2. Material properties

Hardinge Bridge is a historic riveted steel truss bridge built in 1915. Available historical records were used to develop the geometry and structural configuration for the bridge; however, original mill certificates, material-grade specifications or mechanical test results of the existing steel were not available. So, the bridge members are not explicitly assigned a particular steel grade of the past.

Baseline numerical model properties were based on the representative structural-steel properties. The density was assumed to be 7850kg/m³, the Young's modulus (E=200) GPa, the Poisson's ratio 0.30 and the nominal yield strength (Fy=250) MPa. The adopted yield strength represents a representative modelling parameter, and is not to be interpreted as a measured in-situ property of the 1915 bridge steel.

The linear-elastic material formulation was chosen because the goal of the present study is to investigate the structural response and the redistribution of local stresses in the baseline materials under the loading and member-removal scenarios. Long-term deterioration, corrosion, fatigue, residual stress or local damage of the properties of the materials were not explicitly modeled. The calculated response needs thus to be understood conditioned on the adopted material parameters.

In the case of tension members, the axial stress computed was compared with the adopted value of the nominal yield stress. The resistance of compression members was determined not by comparing the compressive stress with the yield strength, but by using the theoretical column buckling formulation presented in Section 2.8.

2.4.3. Boundary condition and load-transfer mechanism

The representative 345-ft (105-m) span was modeled using 3-D nodal coordinates representing the geometry of the bridge as documented. The support conditions were idealized to simulate the longitudinal and transverse restraint from the bridge bearings. Assuming the support conditions, the translational degrees of freedom were restrained and the rotational degrees of freedom were kept if they were necessary as per the beam-column equivalent floor system. The selected boundary conditions have been assumed to be idealized baseline conditions as detailed in-situ bearing stiffness and rotational conditions were not available.

Railway loads were not placed directly on main truss nodes, but on the floor system. Wheel reactions were originally placed at the proper rail/stringer locations, carried along the longitudinal stringers and floor beams and then conveyed to the main truss at the same panel point locations. The position of the train was gradually moved along the span to determine the characteristic response position. The magnitude of the wheel/axle load, wheel spacing, axle spacing, number of loaded axles, and the nodal load values are all given in the updated model description.

2.5. Loading conditions

2.5.1. Dead load

The dead load includes the self-weight of the bridge members and all other superimposed loads which are permanently attached to the structure. Two railroads are present in the bridge and the weight of rail and sleepers are considered as 0.09 kip/ft uniformly distributed load on four stringers of the bridge [21].

2.5.2. Live load

The Live load is considered as train load. Therefore, the wheel arrangement and loading of WDM2 Co-Co type for locomotive and Bo-Bo type for bogies are taken into consideration. The center-to-center spacing of two wheels of Co-Co type locomotive and Bo-Bo type bogie is 6.75 feet and 8.5 feet, respectively [22].

2.5.3. Dynamic load considerations

The railway live-load effects were adopted and a constant dynamic load allowance factor of 1.15 was applied to these in both the intact and member-removal scenarios. This factor is an abridged allowance for dynamic effects involved in mobile loading of the railway and is not a transient dynamic analysis. The dynamics associated with the sudden removal of members were not added. Fig. 2 illustrates an applied loading configuration, which was used in the analysis.

2.6. Structural response analysis

FEM was used to evaluate the principal structural response parameters, including axial stress of steel truss members, displacement of the nodes of the steel truss, member stress distribution and load path distribution. A detailed investigation was conducted of three major fracture situations that occurred at various locations along the span.

2.7. Structural redundancy analysis

Numerical results were analyzed in Python with OpenSeesPy framework. Firstly, an intact model of the bridge was analyzed with the given dead and live loads of the railway. Then, one by one, selected members were removed to simulate member loss in localized areas, and the resulting changes in the axial force and stress of the adjacent members were assessed. Therefore, the analysis is not considered a full-scale system-level redundancy or reliability analysis, but rather a local alternate-load-path assessment based on a deterministic approach.

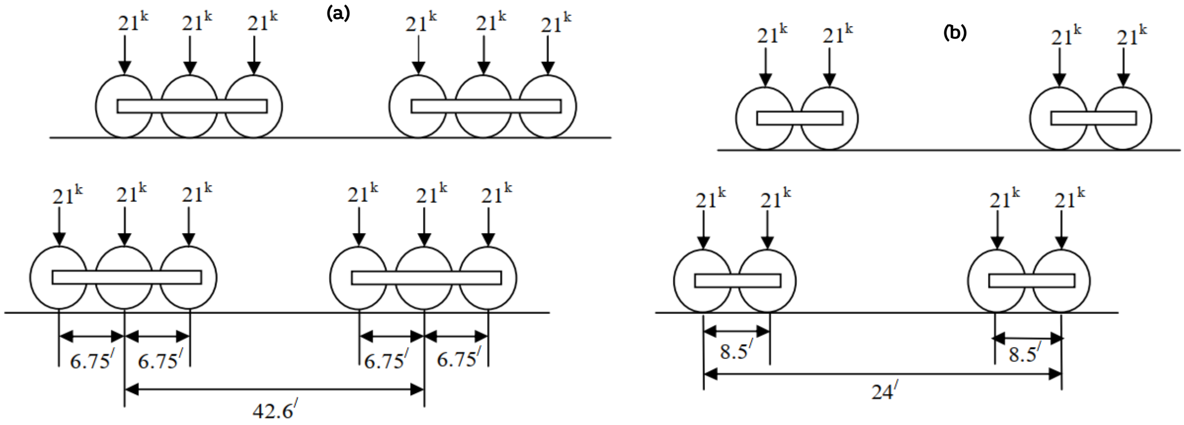

Figure 2. Loadings and wheel arrangements of two types of locomotives (a) Co-Co and (b) Bo-Bo

2.8. Demand/Capacity ratios analysis

Demand-to-capacity (D/C) ratios were determined for those critical members identified in the member-removal simulations. The demand was considered to be the maximum tensile axial stress in tension members extracted from the verified OpenSeesPy analysis and the reference resistance adopted was based on the nominal yield strength of 250MPa.

The theoretical column-buckling resistance was used to calculate the governing resistance, instead of using the yield strength directly, for compression members. The calculation was done as per AISC 360 specification [23]. The idealized baseline assumption of an effective length factor (K=1.0) was used for truss members. This is not intended to be used as a measured effective length condition of an existing bridge as the actual value of the rotational restraint of the historic riveted connections was not available.

D/C ratios of each member were determined by dividing the adopted resistance by the applied demand. A number less than unity means that the calculated demand is less than the adopted resistance in the context of the assumptions of the numerical model. This value does not formally certify the structural safety of the existing bridge.

2.9. Model verification and validation limitations

The size and the structural layout of the representative bridge span was identified based on past information and records. However, the results of field measurements, ambient-vibration data, strain-monitoring records, detailed bearing properties, and direct material-test results were not available for an independent validation of the numerical model. It is thus important to acknowledge that the analysis presented herein is a numerical approximation of a baseline bridge configuration, which may be idealized.

The main restrictions are the following:

- ✓ Since no mechanical-test data were available for the existing steel, the material properties used were representative.
- ✓ Explicitly taken care of in the model are not the section reduction caused by corrosion, fatigue damage, residual stresses, and deterioration of riveted connections.
- ✓ The rotational stiffness and true restraint properties of historic riveted connections and bearings are simplified.
- ✓ Primary truss members are idealized based on their dominant axial response while beam-column elements are used to represent the load transfer in the flexural response for the floor-system members.
- ✓ The railway loading configuration was simplified and the dynamic load allowance was assumed to be constant instead of using a full train–bridge interaction analysis.
- ✓ The baseline analysis is linear elastic and does not include material yielding, geometric nonlinearity, connection failure, or nonlinear progressive-collapse behavior.
- ✓ The member-removal analysis is meant to address the selected localized scenarios and is not to be taken as a system-level redundancy or reliability analysis.
- ✓ The adopted material properties, the effective length factor, the support conditions and the cross-sectional properties have not been quantified in terms of their uncertainty through a formal probabilistic sensitivity analysis.

As such, the results provide a preliminary computational screening of the structural response and local load redistribution. They are not to be considered as a final determination of the safety or serviceability of the existing Hardinge Bridge.

3. Results

3.1. Structural response to train loading

The maximum vertical movement was calculated to be about 4.02 in (102 mm) at mid-span. For a 345-ft (4140-in) span, the corresponding L/1200 and L/1000 values are approximately 3.45 and 4.14 in, respectively. Hence, the computed displacement is greater than L/1200, but less than L/1000. Since the present investigation does not provide a definitive pass/fail serviceability analysis for the historic structure, this result is presented as a numerical comparison.

3.2. Axial stress distribution

The calculated axial stresses of the members investigated varied between −99.5 and 93.4 MPa in the intact model and −86.0 and 64.6 MPa following the member removal scenarios studied (Fig. 3). Member (g) showed a stress change from tension (+17.1 MPa) to compression (−29.1 MPa) after member (h) was removed, which illustrates the redistribution of stresses in the truss.

3.3. Redundancy and member removal analysis

The bridge was modelled and the pertinent loads applied; the whole bridge was then analyzed in its intact state. All members' axial stresses were directly calculated within OpenSeesPy framework. Afterwards, the model was modified by removing a primary member to create a fracture scenario and the analysis was repeated. The remaining members in the fractured configuration were then analyzed using the same applied load to assess load redistribution and redundancy behavior of the remaining members by comparing the axial stresses to that obtained from the intact model. In the present work three critical fracture scenarios at three different positions of the bridge are presented and discussed.

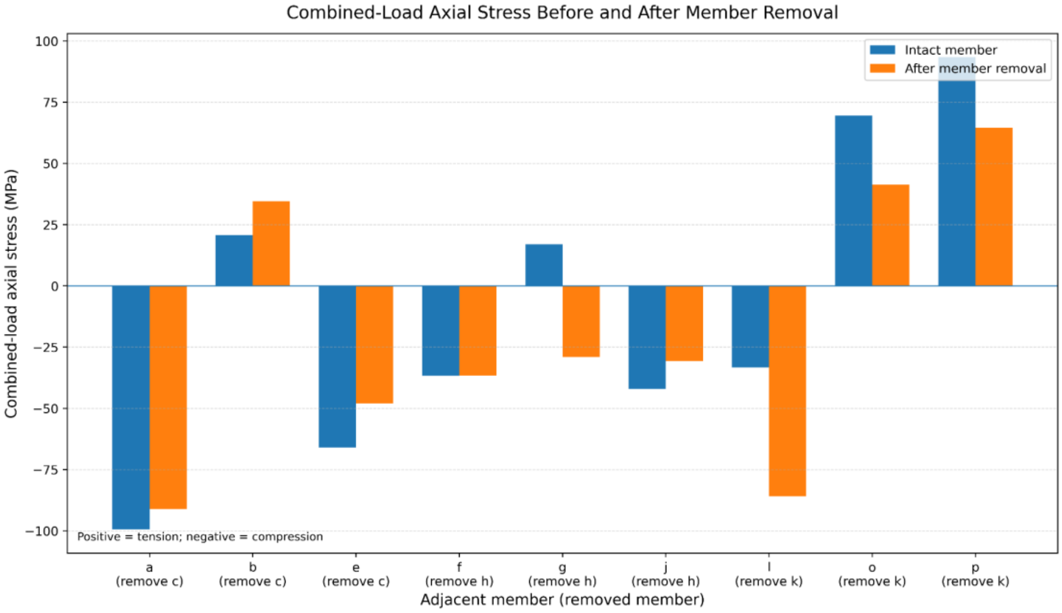

Figure 3. Axial stress distribution in the truss members under combined loading

3.3.1. Removal of member (c)

For the first scenario, it was assumed that the vertical member (c) was fractured. In Fig. 4, the fractured member and surrounding members are shown, with member (d), which is directly connected to member (c), having no force on it after the fracture. Table 1 shows the axial stresses of the adjacent members (a), (b) and (e) for dead, moving and combined loading condition. Based on the results, it is observed that the axial stress of the member (b) under the dead load condition is approximately 78.6% higher and under the combined loading condition is approximately 66.7% higher. The increase is due to the fact that members (b), (c), (d) and (e) are a single truss unit and if member (c) fails, load equilibrium is lost, and member (d) is ineffective. Thus, the load applied is mostly transferred to member (b). When an extra load is placed on the bridge, localized failure or yielding may occur if the redistributed load exceeds the axial capacity of member (b).

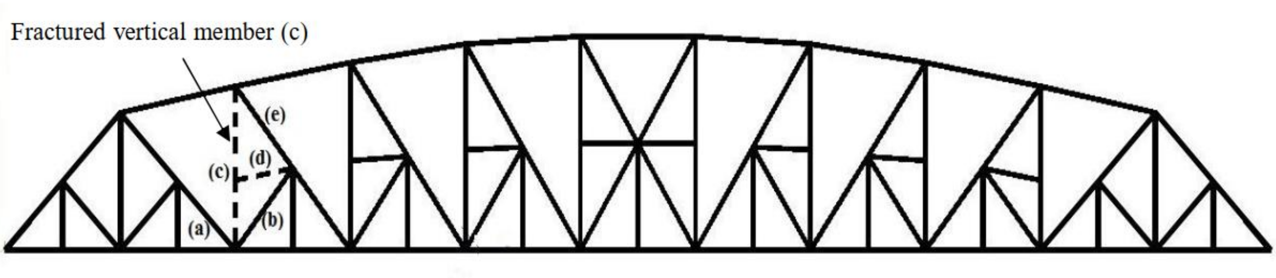

Figure 4. Fractured vertical member (c) and its adjacent members

Table 1. Changes in axial stresses of adjacent members due to removal of member (c)

Member	Stress due to dead load (psi)			Stress due to live load (psi)			Stress due to combined load (psi)		
	Before fracture	After fracture	Percentage	Before fracture	After fracture	Percentage	Before fracture	After fracture	Percentage
(a)	-7994.1	-7263.2	9.1%	-6440.2	-5963.2	7.4%	-14434.3	-13226.4	8.4%
(b)	1416.4	2530.3	78.6%	1594.0	2488.0	56.1%	3010.4	5018.4	66.7%
(e)	-4894.6	-3442.3	29.7%	-4677.1	-3503.5	25.1%	-9571.7	-6945.8	27.4%

*The percentage change is given by $\left(\mid \sigma_{after} \mid - \mid \sigma_{before} \mid\right) / \mid \sigma_{before} \mid \times 100\%$. In cases of stress sign reversals, the percentage change is not regarded as an increase or a decrease in the conventional sense, but rather as an indication of the change from tension to compression and vice-versa.

3.3.2. Removal of member (h)

In this case, it was assumed that vertical member (h) was broken. After the fracture, member (i) has no load, as it is no longer effective, since it is directly connected to the fractured member. The fractured member and adjoining members are shown as in Fig. 5 and the variations of the axial stresses in the adjoining members (f), (g) and (j) for dead load, moving load and combined load conditions are shown in Table 2. The results show that the axial stress of member (g) increases about 70.3% after the fracture of member (h). This behavior is explained by the fact that the members (g), (h), (i), and (j) make up one truss unit and the load equilibrium is affected when member (h) fails, so member (i) is inactive. Thus, the load redistributed will mainly pass-through member (g). The load on member (g) is the load carrying capacity, if the additional load is greater than this, member (g) may exceed its elastic limit, compromising the stability of the adjacent truss panel.

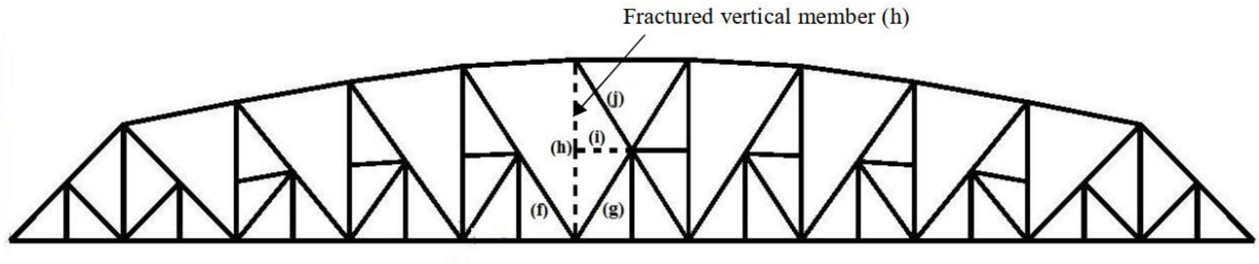

Figure 5. Fractured vertical member (h) and its adjacent members

Table 2. Changes in axial stresses of adjacent members due to removal of member (h)

Member	Stress due to dead load (psi)			Stress due to live load (psi)			Stress due to combined load (psi)		
	Before fracture	After fracture	Percentage	Before fracture	After fracture	Percentage	Before fracture	After fracture	Percentage
(f)	-1585.4	-1596.5	0.70%	-3735.5	-3714.3	0.6%	-5320.9	-5310.8	0.2%
(g)	215.8	-144.9	32.87%	2259.0	-4071.6	80.2%	2474.8	-4215.6	70.3%
(j)	-2016.4	-1474.7	26.86%	-4093.9	-2980.3	27.2%	-6110.2	-4454.9	27.1%

Member (g) showed a stress-state reversal after the removal of member (h). The change in its axial stress during dead load was from +215.8 psi (tension) to -144.9 psi (compression), and the change in the combined-load stress was from +2474.8 psi to -4215.6 psi. This is a more structural transition because it changes the resistance mechanism when the transition from tension to compression occurs in a member. Compression adds an applicable buckling limit state, which does not apply to a member that is tensile only. Hence, the answer is termed as "stress reversal" and is not a conventional percentage increase or decrease.

3.3.3. Removal of member (k)

In this case, it was assumed that diagonal member (k) was fractured and the changes in the axial stresses were compared with stresses in the intact bridge. The broken diagonal member and adjacent members are shown in Fig. 6, in which the dotted lines are inactive members. Table 3 shows the axial stress changes of the neighboring members (l), (o) and (p) for the above three loading conditions: dead load, moving load and combined load.

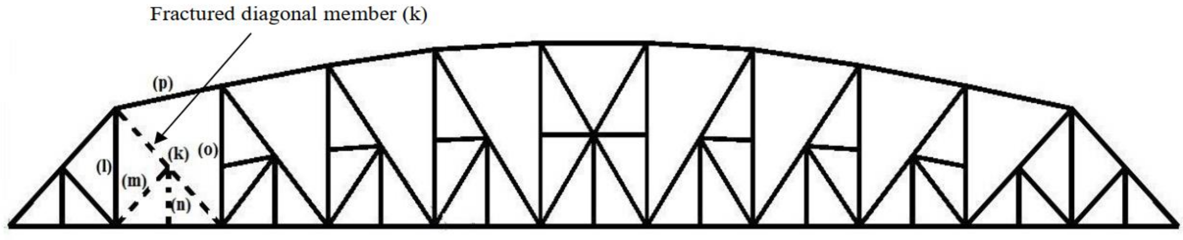

Figure 6. Fractured diagonal member (k) and its adjacent members

Table 3. Changes in axial stresses of adjacent members due to removal of member (k)

Member	Stress due to dead load (psi)			Stress due to live load (psi)			Stress due to combined load (psi)		
	Before fracture	After fracture	Percentage	Before fracture	After fracture	Percentage	Before fracture	After fracture	Percentage
(l)	-1874.2	-5814.1	210.2%	-2954.1	-6652.8	125.2%	-4828.3	-12466.8	158.2%
(o)	5426.3	2930.1	46.0%	4671.5	3074.1	34.2%	10097.7	6004.1	40.5%
(p)	7879.4	5450.1	32.5%	5671.2	3924.2	30.8%	13550.6	9374.3	30.8%

The results show that after the member (k) is broken, the load in member (l) increases by a factor of 210.2% if it is subjected to dead load alone, and by a factor of 158.2% if it is subjected to both dead load and live load. This significant rise is due to the disintegration of the truss unit consisting of the members (k), (l), (m) and (n). The members (m) and (n) are directly connected to the fractured member and so they too lose their effectiveness leading to a significant load re-distribution to member (l). When the load on member (l) is redistributed, if it is still greater than the load-bearing capacity of member (l), it is possible that the structure will suffer a localized loss of load-carrying capacity, necessitating a nonlinear dynamic analysis to fully evaluate the failure mechanism.

3.4. Demand/Capacity ratios

The calculated D/C ratio for the members investigated did not exceed a value of 1 for the resistance adopted as per Table 4 and Table 5. The ratios were calculated using the adopted nominal tensile strength for tension members, and the calculated buckling resistance for compression members. These results suggest the demands calculated in the idealized model did not exceed the adopted resistance, but these results should not be regarded as a formal certification of the existing bridge.

Table 4. D/C ratios based on yield strength

Member	Scenario (Member removed)	Max stress after fracture (psi)	F_y (psi)	D/C Ratio	Status
(b)	Remove (c)	5,018.4	36,260	0.138	D/C <1.0
(o)	Remove (k)	6,004.1		0.166	
(p)		9374		0.259	

Table 5. D/C ratios based on buckling resistance

Member	Scenario (Member removed)	KL/r	F_{cr}(ksi)	Stress (ksi)	D/C Ratio	Status
(a)	Remove (c)	92.6	23.02	13.23	0.574	D/C <1.0
(e)		99.1	21.53	6.95	0.323	
(f)	Remove (h)	113.4	18.35	5.31	0.289	
(g)		121.0	16.69	4.22	0.253	
(j)		121.0	16.69	4.45	0.267	
(l) (Diagonal)	Remove (k)	81.3	25.53	12.47	0.488	

3.5. Discussion

3.5.1. Structural performance

The calculated mid-span displacement is the response of the idealized baseline model under the loading, geometry, support condition and representative material properties used. The model has not been verified by means of field measurements and the numerical displacement does not necessarily provide evidence of the stiffness of the existing bridge having been maintained through its service life as the deterioration or section loss is not explicitly modeled.

3.5.2. Redundancy implications

Based on the member-removal simulations, it is found that the analyzed truss configuration can redistribute the load after localized member loss. However, the extent of load redistribution depends heavily on the location and type of the removed member. For the investigated members, where large stress increments are found, they can thus be assumed to be highly stressed/load critical in the scenarios analyzed. The present results do not provide evidence of fracture-critical behavior as they do not assess residual capacity, connection failure and nonlinear dynamic response. These members should be given special consideration, however, for future inspection and detailed structural examination.

3.5.3. Implications for management of aging railway bridges

The present computational approach may serve as a preliminary screening tool for identifying bridge regions where localized member loss could produce substantial stress redistribution. Such numerical screening should be complemented by field inspection, material characterization, corrosion/section-loss measurements, connection assessment, and, where feasible, structural health monitoring before decisions concerning rehabilitation or continued service are made.

4. Conclusion

A 3-D finite element model of a typical 345-ft (105-m) span of the historic Hardinge Bridge, Bangladesh was created to examine the structural response and local load redistributions of the bridge when subjected to an idealized railway loading configuration. The model was built in OpenSeesPy, with available historical information on the bridge geometry and structural-steel properties (where no material-test data were present). The baseline analysis resulted in a maximum vertical displacement of ~4.02in (102mm) in the loading configuration used in the analysis, close to the midspan area. This is greater than an (L/1200) comparison value of about 3.45 for the 345-ft span, but lesser than an (L/1000) comparison value of about 4.14 in. It is important to note that no bridge-specific serviceability governing criterion was set in the current study and therefore this comparison should not be viewed as a final pass or fail criterion for the serviceability of bridges. The member-removal simulations showed that there was significant local redistribution of axial demand. In particular, some neighboring members experienced marked increase in stress magnitude and member (g) went from tension to compression after the removal of member (h). This stress reversal will prove to be important since the potential governing limit state shifts from tensile to compression-related stability. In the idealized numerical model, the investigated members were below the theoretical buckling resistance or adopted yield. The calculated D/C ratios should not, however, be considered to be formal safety factors or a reflection of the current safety of the existing bridge. This analysis is a first order calculation and is deterministic with no field validation, deterioration-based loss of section, material degradation, detailed riveted-connections behavior, nonlinear material behavior, geometric nonlinearity or dynamic member-removal effects. The study is therefore very useful as a starting point in calculating structural response and potential alternate load paths in an historic railway truss as a preliminary computational screening. Future tasks should include field measurements, material characterization, corrosion and section-loss data, connection level modelling, systematic member removal screening, sensitivity/uncertainty analysis and nonlinear static/dynamic simulation to develop a more complete assessment of the bridge's residual structural capacity.

Author Contributions

M.S.R.: Conceptualization, Investigation, Data Curation, Software, Visualization, Writing – Original Draft.

M.M.R.: Investigation, Data Curation, Validation, Visualization, Writing – Original Draft, Writing – Review & Editing.

N.C.R.: Investigation, Data Curation, Supervision, Visualization, Writing – Review & Editing.

A.K.D.: Conceptualization, Methodology, Data Curation, Software, Writing – Review & Editing.

Funding

This research received no external funding.

Data Availability Statement

The data for this study are available from the corresponding author upon reasonable request.

Declaration of Conflict of Interests

The authors declare that there is no conflict of interest.

References

[1.] Khan, M.S., Caprani, C., Lenner, R., Sýkora, M. Reliability assessment of steel truss railway bridges at ultimate limit state under combined loads (2023).

[2.] Ellobody, E. Finite element analysis and design of steel and steel–concrete composite bridges. Elsevier (2023).

[3.] Bertolesi, E., Buitrago, M., Adam, J.M., Calderón, P.A. Fatigue assessment of steel riveted railway bridges: Full-scale tests and analytical approach. Journal of Constructional Steel Research 182 (2021) 106664.

[4.] Al-Emrani, M., Kliger, R., Al Nuaimi, A. Fatigue assessment of riveted railway bridges: Review and evaluation of current methods. Structure and Infrastructure Engineering 13 (2017) 230–246. https://doi.org/10.1080/15732479.2016.1150906

[5.] Zhao, Y., Deng, L., Li, A. Fatigue damage assessment of steel railway bridges under repeated train loads. Engineering Structures 235 (2021) 112081. https://doi.org/10.1016/j.engstruct.2021.112081

[6.] Deng, L., Li, A., Chen, B. Fatigue reliability analysis of steel railway bridges under train-induced stress cycles. Engineering Structures 254 (2022) 113828. https://doi.org/10.1016/j.engstruct.2022.113828

[7.] Ghosn, M., Moses, F., Frangopol, D.M. Redundancy and robustness of highway bridge superstructures and substructures. Structures and Infrastructure Systems (2019) 376-397.

[8.] Frangopol, D. M., Soliman, M. Life-cycle performance of deteriorating structures: Review. Journal of Structural Engineering 142 (2016) 04016060. https://doi.org/10.1061/(ASCE)ST.1943-541X.0001542

[9.] Li, Y., Chen, Z., Fu, G. Alternate load path method for redundancy evaluation of steel truss bridges. Engineering Structures 206 (2020) 110138. https://doi.org/10.1016/j.engstruct.2019.110138

[10.] Fu, G., You, J. Progressive collapse analysis of truss bridges under member failure. Journal of Bridge Engineering 24 (2019) 04019024. https://doi.org/10.1061/(ASCE)BE.1943-5592.0001360

[11.] Ambroziak, A., Malinowski, M. Structural evaluation of a historic riveted railway truss bridge under modern loading conditions. Baltic Journal of Road and Bridge Engineering, 18 (2023) 45–60.

[12.] Xia, H., Zhang, N., Guo, W. Dynamic interaction of train–bridge systems under moving loads. Engineering Structures 211 (2020) 110426. https://doi.org/10.1016/j.engstruct.2020.110426

[13.] Sohn, H., Farrar, C.R., Hemez, F.M., Czarnecki, J.J. A review of structural health monitoring literature: 1996–2016. Los Alamos National Laboratory (2017).

[14.] Spencer, B.F., Hoskere, V. Advances in computer vision-based civil infrastructure inspection and monitoring. Engineering 5 (2019) 199–222. https://doi.org/10.1016/j.eng.2018.11.030

[15.] Bao, Y., Li, H. Machine learning paradigm for structural health monitoring. Structural Health Monitoring 18 (2019) 1461–1478. https://doi.org/10.1177/1475921718794056

[16.] Azimi, M., Pekcan, G., Jankowski, Ł. Structural health monitoring using machine learning techniques: A review. Mechanical Systems and Signal Processing 147 (2020) 107087. https://doi.org/10.1016/j.ymssp.2020.107087.

[17.] American Association of State Highway and Transportation Officials (AASHTO). LRFD bridge design specifications (9th ed.) (2020).

[18.] Ghosn, M., Moses, F., Wang, J. Design of highway bridges for structural redundancy (NCHRP Report 489). Transportation Research Board (2003). https://doi.org/10.17226/10853

[19.] Fisher, J.W., Kulak, G.L., Smith, I.F.C. A fatigue primer for structural engineers. National Steel Bridge Alliance (1997).

[20.] Zhu, M., McKenna, F., Scott, M.H. OpenSeesPy: Python library for the OpenSees finite element framework. *SoftwareX 7*(2018) 6-11.

[21.] Gupta, B.L., Gupta, A. Roads, Railways, Bridges, Tunnels and Harbour-Dock Engineering (2003).

[22.] Scannel, T., Norgrove, K., Bendall, S., Monk, A., Elliott, R. BR diesel and electric bogie loco wheel and wheelbase information. Central London Area Group of the Scalefour Society (2011).

[23.] AISC Committee. Specification for structural steel buildings (ANSI/AISC 360-10). *American institute of steel construction, Chicago-Illinois (2010)*.

How to Cite This Article

Reza, M.S., Rahman, M.M., Roy, N.C., and Debnath, A.K., Structural Performance and Redundancy Assessment of an Aging Steel Truss Railway Bridge: A Computational Study of Hardinge Bridge, Bangladesh, Civil Engineering Beyond Limits, 1(2027), 11168. https://doi.org/10.36937/cebel.2027.11168